I gratefully acknowledge the hospitality and support of the Royal Melbourne Institute of Technology and Melbourne University during my stay in Melbourne throughout 1985, when most of this work was carried out. The work was also partially supported by JSEP contract no. F49620-85-C-0078.

References

AFANAS'EV, A. M. & PERSTNEV, I. P. (1969). *Acta Cryst.* A**25**, 520-523.

BETHE, H. A. (1928). *Ann. Phys. (Leipzig)*, **87**, 55-129.

EWALD, P. P. & HÉNO, Y. (1968). *Acta Cryst.* A**24**, 5-15.

HERZBERG, B. (1971). *Z. Naturforsch. Teil A*, **26**, 1247-1253.

HØIER, R. & MARTHINSEN, K. (1983). *Acta Cryst.* A**39**, 854-860.

ICHIKAWA, M. & HAYAKAWA, K. (1977). *J. Phys. Soc. Jpn*, **42**, 1957-1964.

JURETSCHKE, H. J. (1982). *Phys. Rev. Lett.* **48**, 1487-1489.

JURETSCHKE, H. J. (1984). *Acta Cryst.* A**40**, 379-389.

JURETSCHKE, H. J. (1986*a*). *Phys. Status Solidi B*, **135**, 455-456.

JURETSCHKE, H. J. (1986*b*). *Acta Cryst.* A**42**, 405-406.

JURETSCHKE, H. J. & BARNEA, Z. (1986). *Phys. Scr.* **33**, 167-168.

JURETSCHKE, H. J. & WAGENFELD, H. K. (1986). *Z. Phys. B*, **62**, 407-411.

Acta Cryst. (1986). A**42**, 456-464

Direct Measurements of the Complex X-ray Atomic Scattering Factors for Elements by X-ray Interferometry at the Daresbury Synchrotron Radiation Source

BY R. BEGUM

Department of Physics, King's College, Strand, London WC2R 2LS, England

M. HART

Department of Physics, The University, Manchester M13 9PL, England

K. R. LEA

Science and Engineering Research Council, Daresbury Laboratory, Warrington WA4 4AD, England

AND D. P. SIDDONS

Brookhaven National Laboratory, Upton, Long Island, New York 11973, *USA*

(*Received* 24 *January* 1986; *accepted* 16 *April* 1986)

Abstract

A scanning X-ray interferometer system [Hart & Siddons (1981). *Proc. R. Soc. London Ser. A*, **376**, 465-482] has been rebuilt for operation at the SERC Daresbury Synchrotron Radiation Source (SRS). The SRS permits an increase in energy resolution by one decade and *simultaneously* an intensity gain of one thousand times, though in practice the solid-state detector employed limited the peak intensity utilized so that experiments which hitherto demanded one month of counting time are now performed at higher spectral resolution in 2-4 h. Absolute measurements are reported of f' and f'' for the K edges of most elements between ^{34}Se and ^{26}Fe and for L edges of ^{79}Au and ^{74}W over energy ranges of about ± 2 keV near absorption edges and scans with better than 1 eV energy resolution of X-ray absorption near edge structure (XANES) and extended X-ray absorption fine structure (EXAFS) spectra near the edges. Over wide energy ranges the results are compared with the most recent calculations of Cromer & Liberman [*Acta Cryst.* (1981), A**37**, 267-268], which are now easily available to workers in the field.

Introduction

The two-beam scanning X-ray interferometer system which we described earlier (Hart & Siddons 1981) has now been rebuilt and is operating routinely at the Science and Engineering Research Council's Synchrotron Radiation Source (SRS) at Daresbury. A few minor changes were required to match the characteristics of the SRS; the interferometer now disperses radiation in the vertical plane. The mechanical response of the scanning system has been improved and the sequencing of the experiment has been altered to match the characteristics of the more intense source.

The interferometry experiment window on line 7 is 53 m from the effective X-ray source which is 12 mm wide and 300 μm high (Hart & Siddons 1982*a*). With a slit height of 300 μm, the angular divergence of radiation on the interferometer is about 2″ which

0108-7673/86/060456-09$01.50

approximately matches the acceptance angle for Bragg reflection in the X-ray interferometer at 1·2 Å wavelength (10 keV energy). A 300 μm slit height gives intensities of $\cdot 10^4$ s^{-1} per mm of slit width (with the SRS operating at 2 GeV, 200 mA), within the reliable operating range of the intrinsic germanium solid-state detector. Clearly, the question of experimental time is dominated by considerations of detector deadtime and gain stability rather than by demands for increased source power. For the energy band available at the station on beam line 7 from the 1·2 T bending magnet, there is no spectroscopic advantage to be gained by the use of double-crystal monochromator techniques. That situation is different now because the interferometry station has been moved to beam line 9 which utilizes the hard synchrotron radiation from the high-field 5 T superconducting wiggler magnet.

The electromagnetic transducer used in our earlier experiments (Hart & Siddons, 1981) caused unnecessary complications in the least-squares refinement of the data since it had a quadratic force/current relationship. We have replaced it in the SRS instrument by a linear drive consisting of an epoxy-bonded rare-earth permanent magnet driven by an air-cored solenoid.

The present data-collection algorithm is closely similar to that used previously in that the electromagnetic drive is used to step-scan the interferometer, 25 intensity samples being taken over two fringes of the lower diffraction order used. The fundamental [arising from diffraction by the (220) planes] and the first harmonic [arising from diffraction by the (440) planes] are separately but simultaneously collected by taking the output of the hyperpure-Ge detector through two separate pulse-height-analyser systems [single multichannel analysers (SCA) or window discriminator type, *not* a multichannel analyser]. The pulses are counted for fixed time periods and the resultant intensity transferred *via* a microcomputer-based experiment controller (Rodrigues & Siddons, 1979) on to floppy discs for later analysis. The use of two SCA's has several advantages over the use of a conventional multichannel analyser (MCA) in this application. Firstly, the deadtime of the total counting chain is dominated by the time constant of the spectroscopy amplifier and detector in use, and is much smaller than the deadtime due to the digitization process used by most MCA's. This allows at least one order-of-magnitude increase in the maximum intensity which can be measured. This is an important point since it is exactly this maximum count rate which limits the rate of data acquisition in the present synchrotron radiation experiments. In experiments such as these, where pulses of only a few amplitudes are to be counted, computer-controlled SCA's run in parallel have advantages in both speed and cost over the more commonly used MCA's. It is worth remarking that in terms of catalogue prices one can buy about ten SCA's, whose channels may be computer-controlled, for the price of one MCA.

Two-beam interference

When two coherent beams with amplitudes A_1 and A_2 and a phase difference Φ interfere the observed intensity is

$$I_0 = A_1^2 + A_2^2 + 2A_1A_2 \cos \Phi. \quad (1)$$

For a perfect rigid X-ray interferometer, or for our scanning interferometer at some value of the magnet current, Φ is fixed. If a sample is put into the second beam the intensity becomes

$$I_s = A_2^2 + A_2^2 \exp(-\mu t) + 2A_1A_2 \exp(-\tfrac{1}{2}\mu t) \times \cos[(2\pi t/\lambda)(1-n_R) + \Phi], \quad (2)$$

where μ is the conventional linear absorption coefficient and n_R is the real part of the refractive index. λ is the x-ray wavelength and t is the sample thickness. If we write the refractive index n as $n_R + in_I$ then, in a conventional notation,

$$n_R = 1 - (e^2\lambda^2/2\pi mc^2V)(Z + f'), \quad (3)$$

$$n_I = \lambda\mu/4\pi = (e^2\lambda^2/2\pi mc^2V)f''. \quad (4)$$

It is obvious that n_R and hence f' can be determined from the phase shift produced by the sample and that n_I and f'' can be determined from the fringe amplitude change $[\exp(-\frac{1}{2}\mu t)]$ introduced by the sample. In laboratory-based experiments the intensities were so low that this was not competitive with simple attenuation measurements. However, at the SRS we obtain quite satisfactory EXAFS and XANES spectra in both f' and f'' at a rate of about 1 min per measurement point in the spectrum.

There are a variety of measurement routes by which n_R and n_I can be determined from (1) and (2). In these experiments we vary the effective phase difference Φ between the interfering beams by translating the analyser of the interferometer. So far this is the only scheme which has produced X-ray fringes of adequate quality for numerical analysis without operator intervention in the data-analysis cycle.

From standard least-squares analysis we obtain the sample phase shift from which f' is determined and the fringe amplitude change from which μ and f'' are determined.

Energy resolution

In practice the energy resolution of our interferometer arrangement is limited by the intrinsic resolution of the 220 silicon Bragg reflection to $\delta E/E = 5{\cdot}6 \times 10^{-5}$ (Beaumont & Hart, 1974) and is coarsened only very slightly by the effect of the angular width of the incident beam. From Bragg's law, the geometrically

determined energy resolution is

$$\delta E/E = -\cot\theta\,\delta\theta$$

where the beam divergence $\delta\theta$, with a slit height of 300 μm at 53 m from the SRS source, is only $1{\cdot}13\times 10^{-5}$ rad (2·33″). Combination of the two contributions in quadrature gives $\delta E = 0{\cdot}37$ eV at 6·2 keV near the Fe K absorption edge, and $\delta E = 1{\cdot}00$ eV at 12 keV near the Se K absorption edge. These are the minimum and maximum energies which we were able to use at the interferometry station on beam line 7 (a normal bending-magnet beam line) of the SRS at 2 GeV electron energy. When theory and experiment were compared, the Cromer–Liberman theoretical values were convoluted with a rectangular window

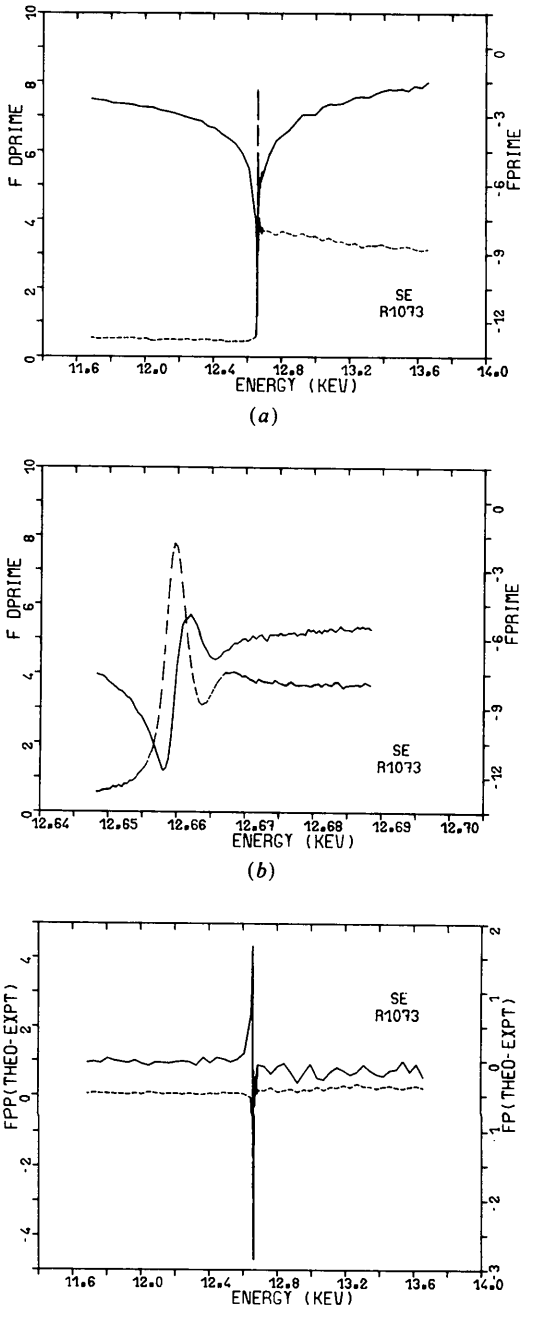

Fig. 1. Dispersion data for selenium. (*a*) Absolute values of f' and f'' over a wide energy range near the K edge. (*b*) Near-edge EXAFS and XANES. (*c*) Comparison with Cromer & Liberman (1981) theory.

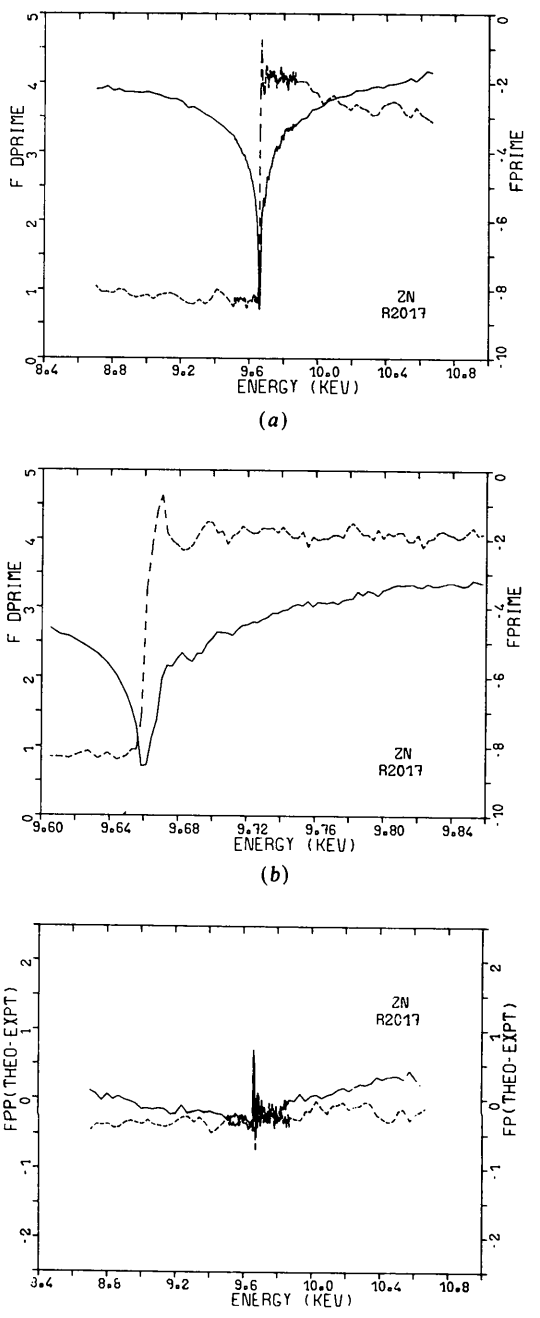

Fig. 2. Dispersion data for zinc. (*a*) Absolute values of f' and f'' over a wide energy range near the K edge. (*b*) Near-edge EXAFS and XANES. (*c*) Comparison with Cromer & Liberman (1981) theory.

function whose width δE corresponded to the interferometer energy resolution.

Experimental results

Measurements near absorption edges obviously involve high sample absorption. In practice the sensitivity of our measurements is limited by counting statistics and interference-fringe contrast with the result that metal foils for K-edge measurements (with $\mu t \sim 1$–2 on the high-energy side of the absorption edge) must be 10–20 μm thick. The X-ray phase advance is about 4π in such foils. For L edges foils must be only ~5 μm thick and the total phase advance is less than 2π.

We have not yet been able to obtain suitable

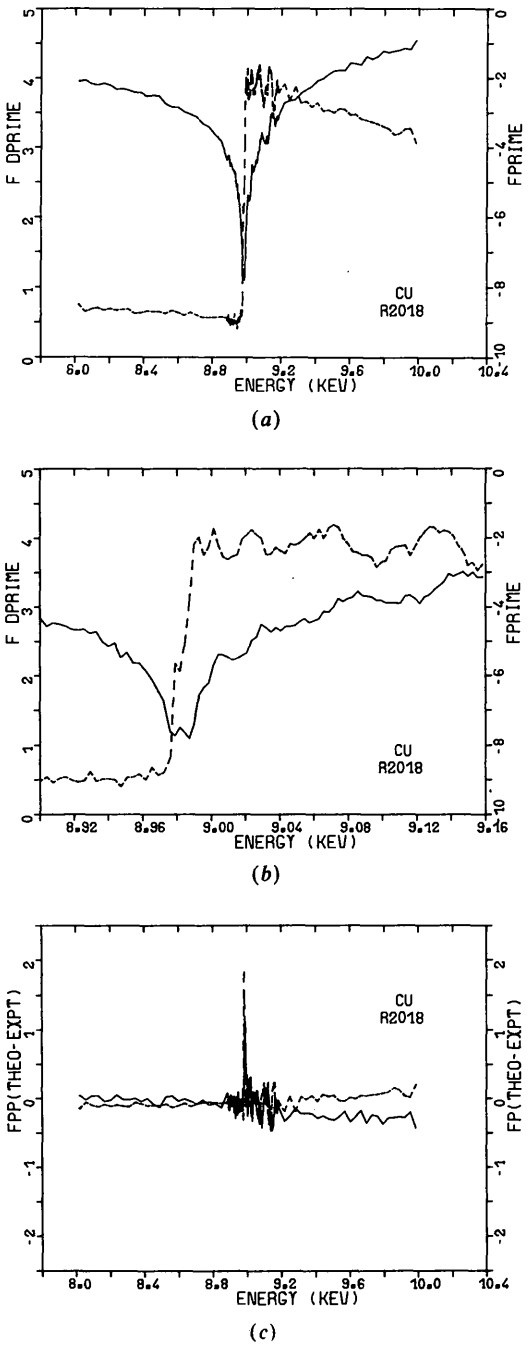

Fig. 3. Dispersion data for copper. (*a*) Absolute values of f' and f'' over a wide energy range near the K edge. (*b*) Near-edge EXAFS and XANES. (*c*) Comparison with Cromer & Liberman (1981) theory.

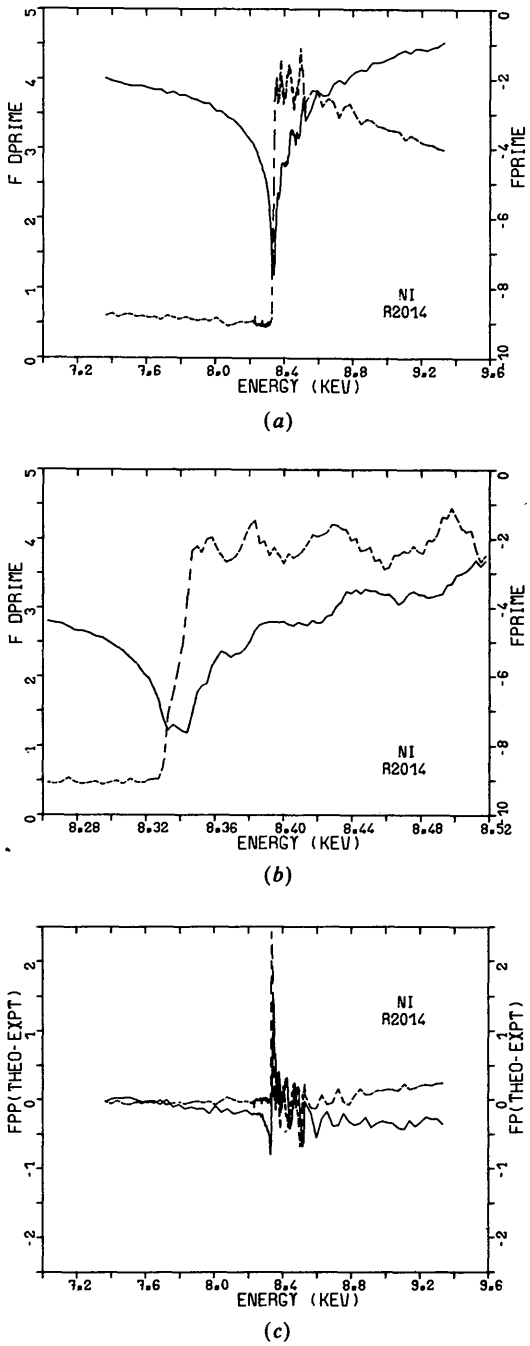

Fig. 4. Dispersion data for nickel. (*a*) Absolute values of f' and f'' over a wide energy range near the K edge. (*b*) Near-edge EXAFS and XANES. (*c*) Comparison with Cromer & Liberman (1981) theory.

samples of ^{33}As, ^{32}Ge and ^{31}Ga, but all the remaining elements from ^{34}Se to ^{26}Fe have been measured near their K edges and some L edges of ^{79}Au and ^{74}W have been studied. Amorphous selenium was obtained from R. Teworte (Univ. of Dortmund) and is the same material as that partially examined by Bonse, Spieker, Hein & Materlik (1980) in Hamburg. All other samples were purchased from Goodfellow Metals Ltd.

Each spectrum was measured in three stages: starting about 1 keV below the absorption edge the interferometer is stepped at approximately 4 eV intervals; near the edge the steps are about five times smaller and on the high-energy side of the absorption edge

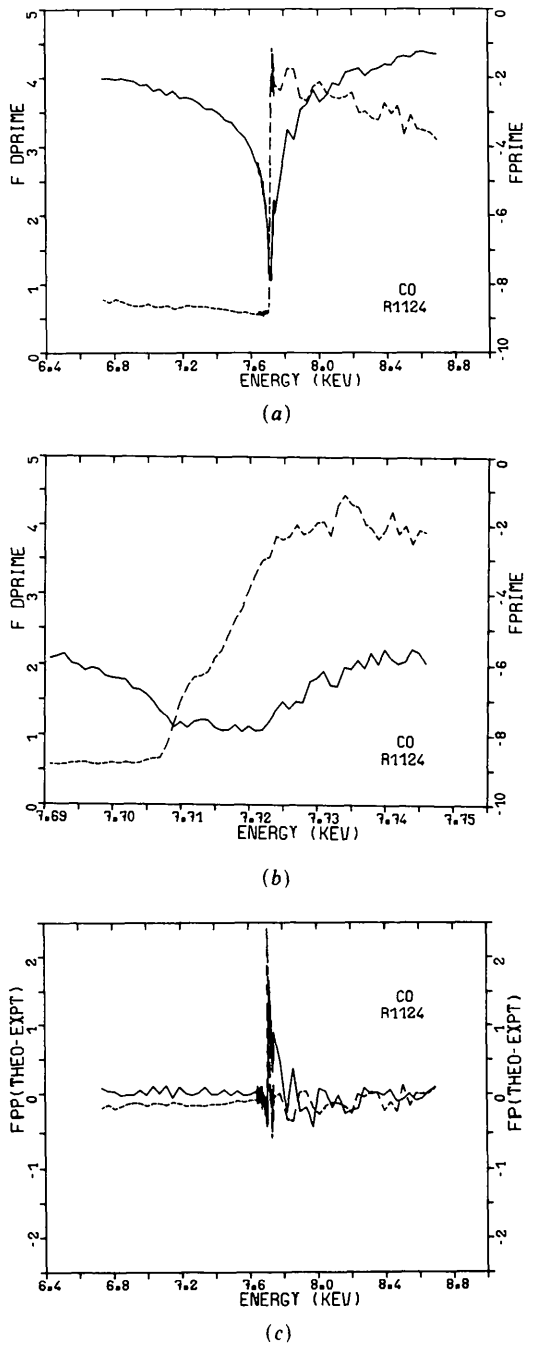

Fig. 5. Dispersion data for cobalt. (*a*) Absolute values of f' and f'' over a wide energy range near the K edge. (*b*) Near-edge EXAFS and XANES. (*c*) Comparison with Cromer & Liberman (1981) theory.

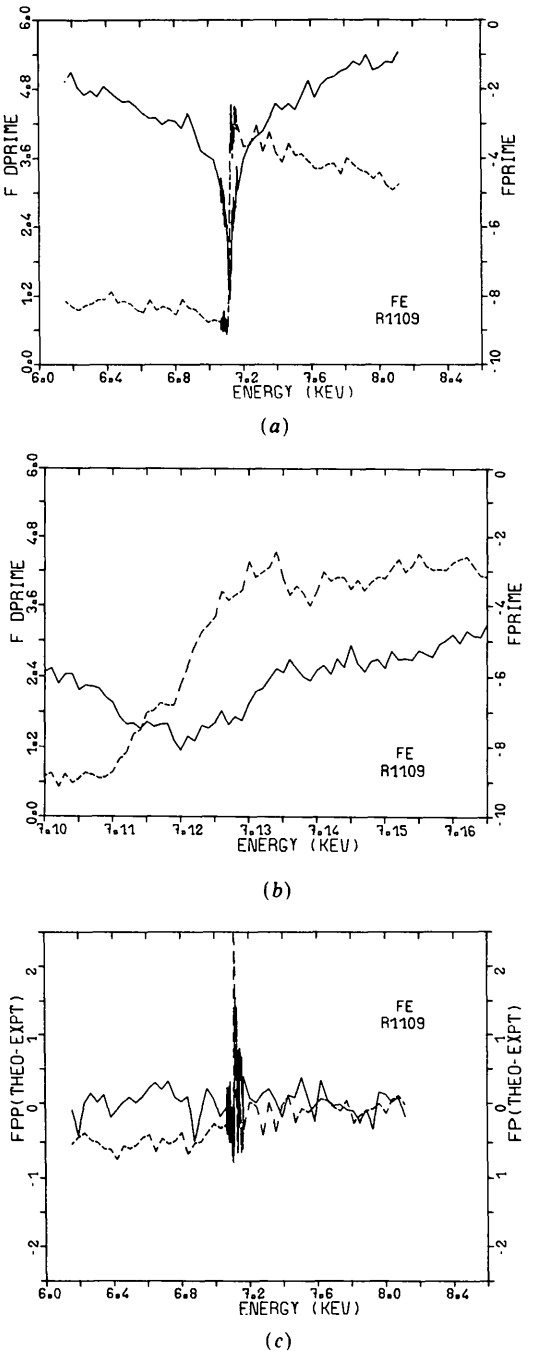

Fig. 6. Dispersion data for iron. (*a*) Absolute values of f' and f'' over a wide energy range near the K edge. (*b*) Near-edge EXAFS and XANES. (*c*) Comparison with Cromer & Liberman (1981) theory.

we revert to the coarse scan. In this way we achieve in a single measurement cycle both wide-energy-range absolute data for comparison with theory and high-resolution data showing EXAFS and XANES near the absorption edge.

Figs. 1–6 show a representative group of *K*-edge spectra each obtained in about two hours with the least-squares data analysis completed without operator intervention; *i.e.* all data are shown with no smoothing, no filtering of source or environmental noise and *no* adjustable parameters. In each figure (*a*) shows f' and f'' over a 2 keV range including the *K* edge, (*b*) shows at high resolution the fine structure in f' and f'' close to the absorption edge and (*c*) shows the difference between our experimental results and Cromer & Liberman's (1981) free-atom theory. Since Cromer & Liberman have published the results of their atomic cross-section theory on magnetic tape, part (*c*) of these figures together with their results permit a complete reconstruction with adequate resolution of our data. These differ slightly in the case of Cu and Ni from previous results (Hart & Siddons, 1982*b*) owing to an inadequate approximation to the harmonic f' in the earlier data analysis: in these experiments we have used Cromer & Liberman's values of f' at the harmonic energy for calibration purposes rather than a simpler approximation.

Figs. 7 and 8 show similar results for the three *L* edges of tungsten metal.

General conclusions

All the *K*-edge dispersion curves can be superimposed within about half an electron (except in the

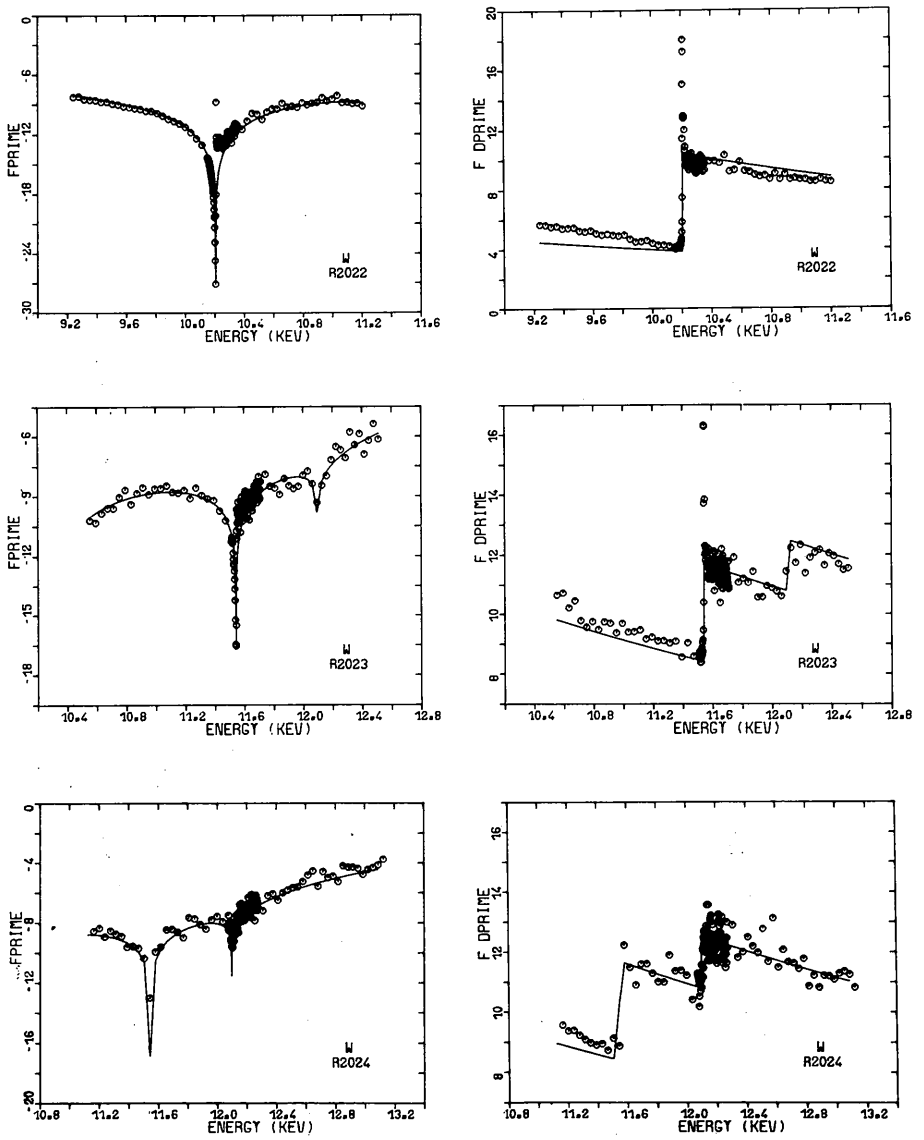

Fig. 7. Dispersion data for the three *L* edges of tungsten.

near-edge region) showing the reliability of our measurements and the expected insensitivity of free-atom K-electron dispersion to atomic number. Most of these f' dispersion curves have never been measured before but our measurements of near-edge structure in f'' [Figs. 1(b)-6(b), 7 and 8] agree with those published during the last 50 years. Interferometric spectra have previously been obtained only for selenium at a few energies (Bonse *et al.*, 1980) and for copper, nickel and cobalt close to the K edge (Bonse, Hartmann-Lotsch & Lotsch, 1982; Bonse & Hartmann-Lotsch, 1984).

It is clear from the difference spectra [Figs. 1(c)-6(c), 8] that the dominant source of systematic error now lies in the sample preparation. Sample surface roughness has a smaller influence on phase shift

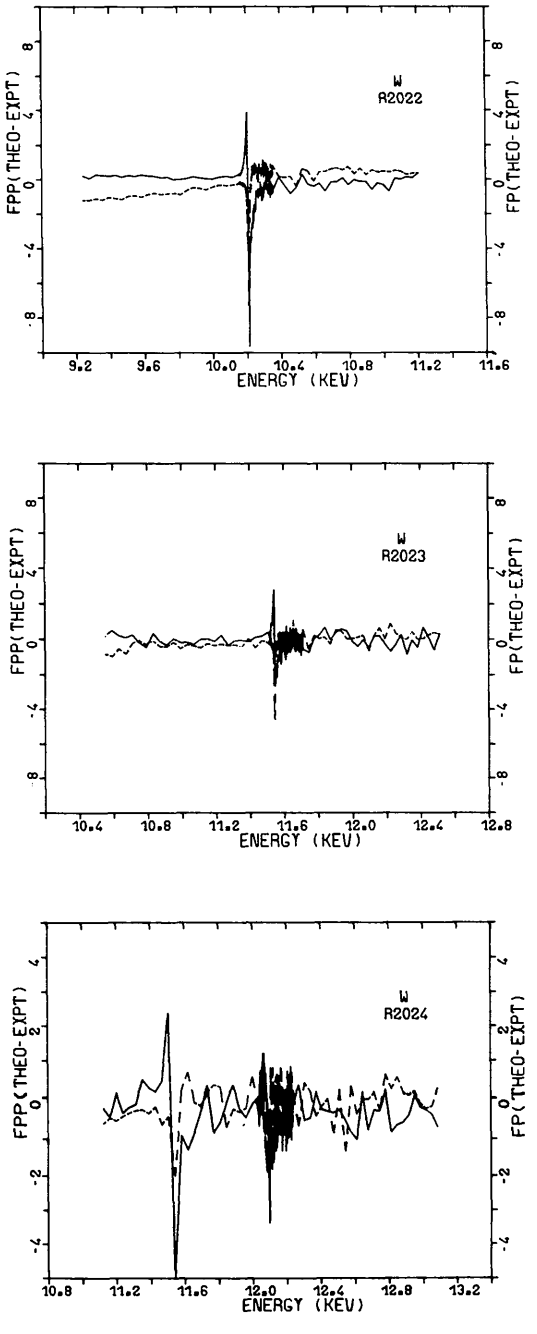

Fig. 8. Comparison of experiment and Cromer & Liberman's (1981) theory for f' and f'' near the tungsten L edges.

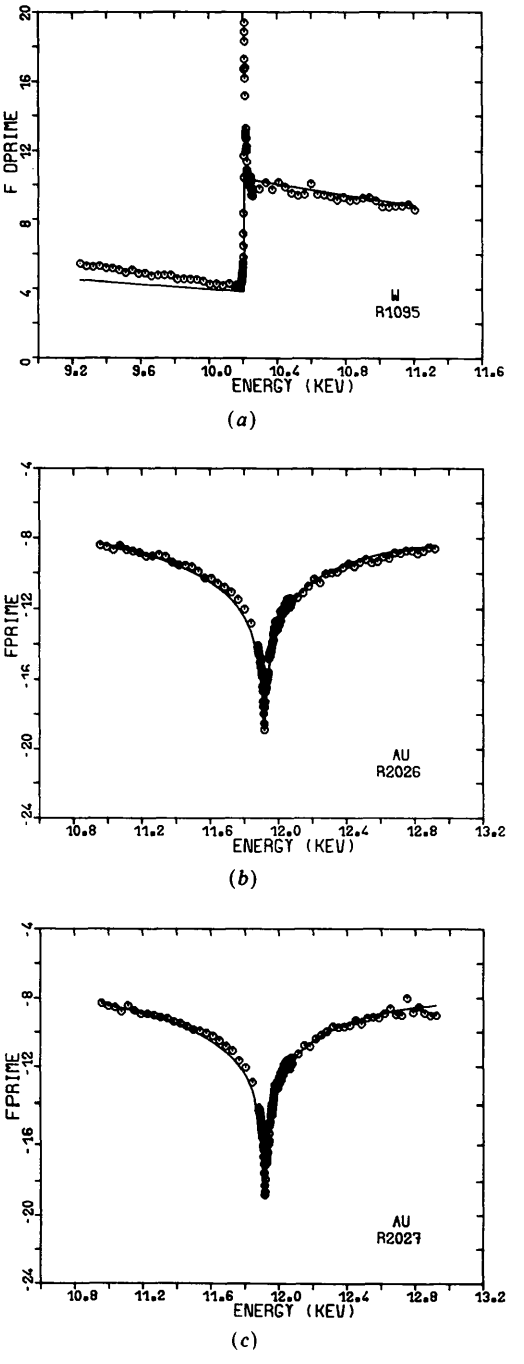

Fig. 9. (a) Repeat of one tungsten L edge; compare with Fig. 7. (b), (c) Two data sets near the gold L_{III} edge showing excellent repeatability.

measurements (f') than on intensity measurements (f'') and it is clear in most of the dispersion spectra that the deviation between theory and experiment is greatest on the high-absorption high-energy side of edges. In the case of the smoothest sample (selenium, Fig. 1) theory and experiment are in precise agreement at low energies and agree within 0·1 electrons for f' and for f'' on the high-energy side of the K edge. In the worst case of the tungsten L edges where the sample is extremely thin and the foil not very smooth (Figs. 7 and 8) the agreement is still within about 0·2 electrons for f' whereas the absorption data (f'') vary, sometimes systematically with energy, by up to ten times as much. Because f' and f'' *must* be related through the Kramers–Kronig transform it follows that some of our data sets, for example the tungsten f' and f'' spectra, are internally inconsistent. We believe that the surface roughness of the metal foil is responsible and that this compromises the measurement of f''. Our results demonstrate too that if one needs to know f' then one should measure f' rather than attempt to perform a Kramers–Kronig transformation on measured f'' data, unless the quality of the sample preparation is beyond question.

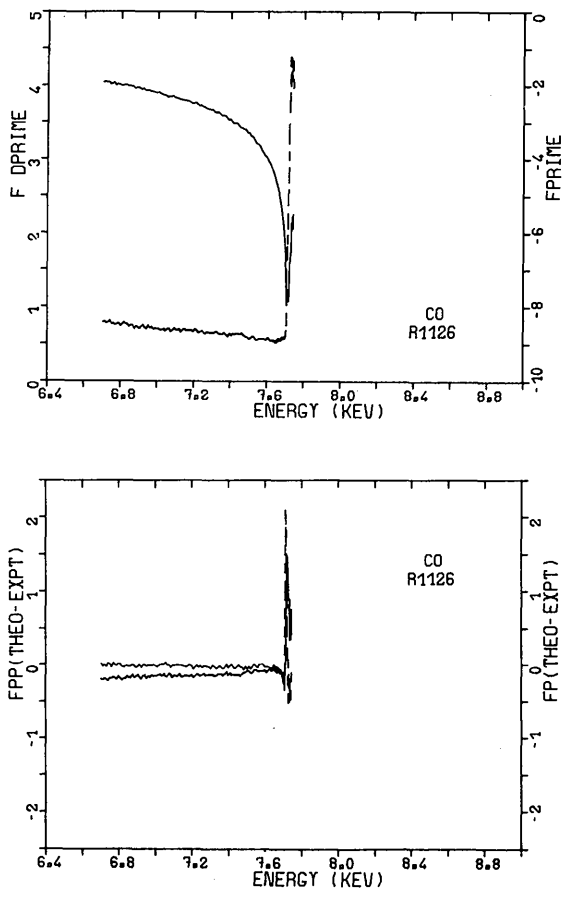

Fig. 10. Best performance to date obtained for a thick cobalt sample on the low-energy side of the K edge.

Systematic errors and further improvements

The spectra published here comprise only a small part of our measured data but suffice to show that X-ray interferometers can produce high-quality data routinely using synchrotron radiation sources. All the spectra shown here have been measured more than once with excellent reproducibility; a second independent set of spectra for selenium, zinc, copper, nickel, cobalt and iron [Fig. 1(A) to 6(A)] has been deposited under the supplementary publication scheme of the International Union of Crystallography.* Fig. 9 illustrates the reproducibility obtained in the unfavourable case of L edges. In f'', Fig. 9(a) shows a spectrum obtained several months after those in Fig. 7 on a different piece of tungsten foil (from the same sheet of as-delivered material). Two independent runs near the gold L_{III} edge made during successive shifts show excellent reproducibility in our f' measurements.

Our experiments were limited in precision by sample preparation and ultimately by counting statistics. That limit is set not by the source (we use a 300 μm × 1 mm beam at 53 m distance with no condensing optics!) but by the detector peak counting rate and the total time set aside for the experiment (2–3 h in the present cases). Fig. 10 illustrates our best achievement showing a fourfold improvement over the 'standard' experiments [compare, for example, with Fig. 5(c) for cobalt]. The deviation from Cromer & Liberman's theoretical result is only ±0·01 electron units in f' away from the K edge but varies systematically with energy and by up to 0·2 electron units in f''. As indicated before, we believe that sample artefacts will cause errors in f'' rather than in f'.

This work was started when three of the authors (RB, MH and DPS) were at King's College in London and has also been supported by the Science and Engineering Research Council.

* Copies of these additional figures have been deposited with the British Library Document Supply Centre as Supplementary Publication No. SUP 42874 (8 pp.). Copies may be obtained through The Executive Secretary, International Union of Crystallography, 5 Abbey Square, Chester CH1 2HU, England.

References

BEAUMONT, J. H. & HART, M. (1974). *J. Phys. E*, **7**, 823–829.

BONSE, U. & HARTMANN-LOTSCH, I. (1984). *Nucl. Instrum. Methods*, **222**, 185–188.

BONSE, U., HARTMANN-LOTSCH, I. & LOTSCH, H. (1982). *EXAFS and Near Edge Structure*, edited by A. BIANCONI, L. INCOCCIA & S. STIPCICH, pp. 376–377. Berlin: Springer.

BONSE, U., SPIEKER, P., HEIN, J.-T. & MATERLIK, G. (1980). *Nucl. Instrum. Methods*, **172**, 223-226.

CROMER, D. T. & LIBERMAN, D. A. (1981). *Acta Cryst.* A**37**, 267-268.

HART, M. & SIDDONS, D. P. (1981). *Proc. R. Soc. London Ser. A*, **376**, 465-482.

HART, M. & SIDDONS, D. P. (1982*a*). *Nucl. Instrum. Methods*, **204**, 219-221.

HART, M. & SIDDONS, D. P. (1982*b*). *EXAFS and Near Edge Structure*, edited by A. BIANCONI, L. INCOCCIA & S. STIPCICH, pp. 373-375. Berlin: Springer.

RODRIGUES, A. R. D. & SIDDONS, D. P. (1979). *J. Phys. E*, **12**, 403-406.

Acta Cryst. (1986). A**42**, 464-469

Secondary Extinction in an Anisotropic Crystal

BY TAKUYUKI S. URAGAMI

Faculty of Science, Okayama University of Science, Ridai-cho, Okayama, 700 Japan

(*Received* 18 *February* 1986; *accepted* 16 *April* 1986)

Abstract

The formalism for secondary extinction developed by Kato [*Acta Cryst.* (1976), A**32**, 453-457, 458-466] is extended to apply to a crystal with anisotropic strain. If an anisotropic correlation for the lattice phase factors is assumed, the formalism can be developed in the same way as for an isotropic crystal. If the geometric average of the correlation lengths of the phase factors is sufficiently smaller than the extinction distance, the ensemble averages of the intensity fields satisfy a set of energy-transfer equations of the same form as in an isotropic crystal. The distribution function of the deviation angle from the exact Bragg condition for the misorientation model of a crystal is given using the notation introduced by Coppens & Hamilton [*Acta Cryst.* (1970), A**26**, 71-83].

1. Introduction

By using the approximation of secondary extinction developed by Zachariasen (1967), Coppens & Hamilton (1970) have shown that anisotropic extinction is often significant in the refinement of a crystal structure. They presented the formalism for two extreme cases: an anisotropic Gaussian mosaic spread distribution function was assumed for a crystal in which extinction is dominated by mosaic spread, and the average particle shape was described as an ellipsoid for a crystal in which extinction was dominated by particle size.

Becker & Coppens (1973, 1974*a*,*b*) developed a formalism for extinction to remove several inadequacies of the theory of Zachariasen, and then (Becker & Coppens, 1975) extended it to include a crystal of non-spherical shape and also to take into account the anisotropy of mosaic spread and particle size introduced by Coppens & Hamilton.

Becker & Coppens assumed incoherent manyfold rescattering of the beams inside a crystal as an approximation in their theory, but extinction theory is based on the dynamical theory of waves in a crystal, and incoherence is treated by taking a statistical average over the crystal. Assuming that the intensity was given by an ensemble average of the intensity field over a statistical ensemble of distorted crystals, Kato (1976*a*,*b*) proposed a formalism to take the statistical nature of lattice distortions into account. The intensity field in his formalism is calculated from the dynamical theory for a distorted crystal developed by Takagi (1962, 1969).

The formalism developed by Kato is extended to include anisotropy in a crystal in the present paper. If an anisotropic and homogeneous correlation of the lattice phase factors is assumed, the formalism can be developed in the same way from the dynamical theory. The distribution function of the deviation angle from the exact Bragg condition for the misorientation model for a crystal which has elastic strains is given using the notation introduced by Coppens & Hamilton (1970).

2. The correlation of the lattice phase factors

We can calculate the wave field of X-rays in a deformed crystal by a pair of partial differential equations derived by Takagi (1962, 1969),

$$\partial d_o/\partial s_o = i\kappa_{-g} \exp(iG) d_g, \qquad (1a)$$

$$\partial d_g/\partial s_g = i\kappa_g \exp(-iG) d_o, \qquad (1b)$$

where d_o and d_g are the wave fields of the transmitted and diffracted waves, respectively, which will be called o and g waves hereafter, s_o and s_g are the oblique coordinates in real space, the axes of which are taken along the directions of the o and g beams, respectively, and κ_g is the reflection strength,

0108-7673/86/060464-06$01.50